BIOPHYSICAL CORTICAL COLUMN MODEL FOR OPTICAL SIGNAL ANALYSIS

S. Chemla
Odyssee Project
INRIA Sophia-Antipolis
2004, route des Lucioles, 06902
Sophia-Antipolis, France
email: sandrine.chemla@sophia.inria.fr

T. Vieville and F. Chavane
Cortex Project/DyVA Team
INRIA Sophia-Antipolis/INCM CNRS
Sophia-Antipolis/Marseille, France
email:Thierry.Vieville@sophia.inria.fr
email: Frederic.Chavane@incm.cnrs-mrs.fr

ABSTRACT
We propose a biological cortical column model, at a mesoscopic scale, in order to better understand and interpret biological sources of voltage-sensitive dye imaging signal (VSD signal). This scale corresponds to one pixel of optical imaging: about 50 μm. Simulations are done with the NEURON software and visualization with the NEUROCONSTRUCT software. This model confirms and quantifies the fact that the VSD signal is the result of an average from multiple components but shows surprisingly that inhibitory cells, spiking activity and deep layers likely participate more to the signal than initially though.

KEY WORDS
Voltage-sensitive dye imaging (VSDI), cortical column, membrane potential, model, NEURON software, NEUROCONSTRUCT software.

1 Introduction

Optical imaging entails new imaging techniques that allow us to visualize the functioning brain at high spatial and temporal resolutions. Specifically, there are two techniques; the first is based on intrinsic signals, and the second is based on VSDs. We consider only the latter. This technique allows to optically image electrical activity. The dye molecules, applied at the surface of the cortex, bind to the external surface of cell membranes and act as molecular transducers that transform changes in membrane potential into optical fluorescence. This optical signal is recorded by a fast camera and displayed as dynamical maps. The amplitudes of the VSD signals are linearly correlated with changes in membrane potential per unit of membrane area of the stained neuronal elements[1]. Indeed, whole cell voltage recordings [2], show a close correlation between individual neurons and the VSD signal. Is this linearity still true for a population of neurons? Which factors can influence this global linearity? Since the VSD signal reflects the summed intracellular membrane potential changes of all the neuronal elements at a given cortical site, this signal is then multi-component: a detailed biophysical model of cortical column is necessary to determine the different contribution of the signal. More precisely, we wish to answer the following questions: what is the participation of the various neuronal components to this population signal? In particular, are excitatory and inhibitory cells participating equally for different levels of activity? Is the ratio between spiking and synaptic activity the same when the network is at low, versus high levels of activity? What are the respective participation of cells from lower versus upper layers?

In this article, we first describe the proposed model of cortical column chosen to analyze biological sources of the optical signal, then we discuss its behavior and its application for VSD signal computation.

2 Methods

2.1 Cortical column controversy

Since the 1950s, thanks to the work of Vernon B. Mountcastle [3], we know that the cerebral cortex has a columnar organization. In 1960s and 1970s, David H. Hubel and Torsten Wiesel ([4], [5], [6]) followed Mountcastle's discoveries by showing that ocular dominance and orientations are organized in a columnar manner in cat and monkey visual cortex. Today, the notion of cortical column becomes a large controversy since the original concept (discrete structure spanning the layers of the somato-sensory cortex, which contains cells responsive to only a single modality) is expanding, year after year, discovery after discovery, to embrace a variety of different structures, principles and names. A 'column' now refers to cells in any vertical cluster that share the same tuning for any given receptive field attribute (see [7] for a detailed review on the cortical column concept). An useful concept is to propose that each definition of cortical column depends on its type (anatomical, functional, physico-functional) and its spatial scale.

Thus, we introduced a new distinction of a cortical column whose the spatial scale is about 50 μm, corresponding to one pixel of optical imaging. Given this spatial scale, the number of neurons, that has been evaluated from [8], is about 180.

2.2 Single neurons

For each neuron, we used a compartmental description with conductance-based Hodgkin-Huxley neuron model. Thus, the dynamics of single cells are described by:

$$\mathbf{C}\,\frac{\mathrm{d}V}{\mathrm{d}t} = \mathbf{I}_{ext} - \sum_i \mathbf{G}_i(\mathbf{V})\,(\mathbf{V} - \mathbf{V}_i) \qquad (1)$$

where $\mathbf{i}$ represents three types of current: leak, potassium and sodium concuctances or respectively $\mathbf{G}_L$, $\mathbf{G}_K$ and $\mathbf{G}_{Na}$. $\mathbf{G}_L$ is independent of $\mathbf{V}$ and determines the passive properties of the cells near resting potential. The sodium and potassium conductances are responsible of the spike generation.
Furthermore, a slow potassium conductance (called M-conductance) was included in the dynamics of the excitatory population to reproduce the observed adaptation of the spike trains emitted by these neurons [9]. This feature seems to be absent in inhibitory neurons.
At the moment, only passive dendrites are considered and each neuron has 7-9 comparments.

2.3 Network Architecture and Synaptic Interactions

We chose a family of models based on a cortical microcircuit, whose synaptic connections are made only between six specific populations of neurons: two populations (excitatory and inhibitory) for three main layers (2/3, 4, 5/6). Thanks to the NEURON software (see the next paragraph) and the ModelDB resource, we have been able to reconstruct four types of neurons [10]: small pyramidal cells in layer 2, spiny stellate cells in layer 4, large pyramidal cells in layer 5 and smooth stellate cells in all layers.
More precisely, the chosen model is a model of 180 neurons, 143 excitatory neurons: 50 small pyramidal (SP) in layer 2, 45 spiny stellate (SS) in layer 4, 48 large pyramidal (LP) in layer 5/6, and 37 inhibitory neurons of one unique type: respectively 14, 13, 10 smooth stellate in layers 2, 4, 5/6 (SmS2, SmS4, SmS5). The number of synapses involved in the projections between these different neuronal types, including the afferent from the LGN (X/Y), were recalculated based on [11] for the considered layers and latencies have been introduced for each connection, following [12].
Synaptic inputs are modeled as conductance changes. AMPA and GABA synapses are respectively converging on dendrites and soma of our neurons.

2.4 Input and Background activity

We simulated input signals from the thalamus into the neocortex layer IV by applying random spike trains to each neuron in layer IV. We then increased the frequency of the spike trains in order to represent stimulus contrast and see how the model transforms an increasing input.

At this point, the column is isolated. We wanted however to reproduce conditions relative to a larger network in order to be realistic. One approach is to simply introduce "background noise" in each neuron of the column. Typically, noise can be introduced in the form of stochastic fluctutation of a current or an ionic conductance. The stochastic model of Destexhe and his collaborators [13], containing two fluctuating conductances, allows us to simulate synaptic backgroung activity similar to in vivo measurements.

2.5 About NEURON and NEUROCONSTRUCT simulation environments

The NEURON software (http://neuron.duke.edu) provides tools for constructing, exercising and managing simplified up to realistic models of electrical and chemical signaling in neurons and networks of neurons. It allows to create and use models of neurons and networks of neurons by specifying anatomical and biophysical properties and by controlling, displaying and analyzing models and simulation results. The main idea of this software is that a physical system which is often very complex can be simplified into a conceptual model which then becomes an abstraction. This conceptual model can then be accurately represented by a computational model. The other main idea is the principle of compartmentalization [14].

We also use the NEUROCONSTRUCT software (www.neuroConstruct.org), that has been designed to simplify development of complex networks of biologically realistic neurons, i.e. models incorporating dendritic morphologies and realistic cell membrane conductances. It is also very useful for the visualization and results analysis.

3 Results

3.1 Model behavior

3.1.1 Single Neurons

We adjusted the intrinsic behavior of our isolated neurons to reproduce those shown in [9] by in vivo intracellular recordings. For each neuron, the parameters to optimize were the channel conductances, the specific axial resistance and the specific capacitance. The optimization algorithm used was the PRAXIS (principal axis) method described by Brent [15]. Fitting a model to a set of data points involves minimizing the deviation of the model's predictions from the data points, thereby allowing us to choose the best parameters and to validate our neurons intrinsic behavior. Figure 1 shows examples of action potential responses to depolarizing current injection in the two main populations of cortical neurons of our model. Regular spiking and fast spiking cells are known to be respectively the great majority of excitatory and inhibitory

cells in the neocortex [16].

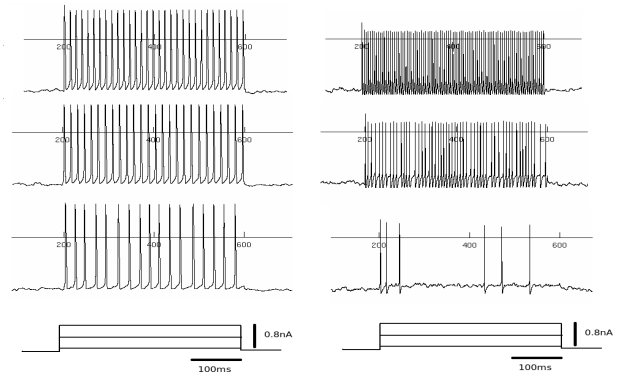

Figure 1. Examples of action potential responses to depolarizing current injection in the two main classes of cortical neuron of our model, fitted with intracellular recording from [9]. *Left*: regular spiking (RS) cell. *Right*: fast spiking (FS) cell.

From these action potential reponses, we calculated the relationship between injected current intensity (in nA) and the total firing rate (in spikes per second). The slope (in Hz/nA) of the linear regression characterizes the current-frequency relationship of the neuron (see Figure 2), which is one of the useful charateristics in distinguishing between different types of neurons [9], especially RS and FS cells. This slope is considerably steeper in the FS cell (300 Hz/nA) compared with that for the RS cell (83.3 Hz/nA), similar to those shown in [9].

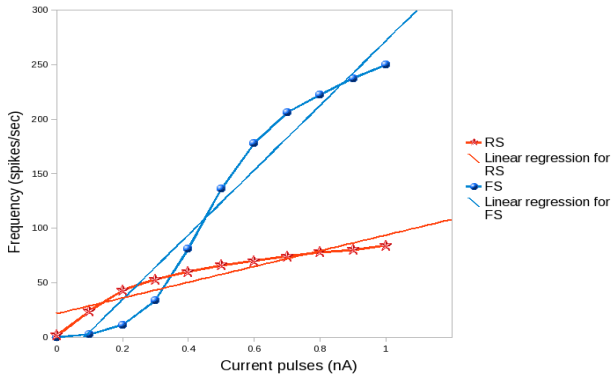

Figure 2. Firing rate vs. current intensity (f-I curves) for the cells shown in Fig. 1. Each point is the average of the mean firing rate for 5 repetitions of a given current intensity.

3.1.2 Network

The next step in the validation of the model is to analyse the behavior of an entire connected network of neurons. To calibrate the network, we chose to compare contrast reponse function (CRF) predicted by the model with those of V1 neurons classically obtained electrophysiologically [16]. Cortical cells adjust non-linearly their response to an input with increasing strength, described by the contrast response function [17]. Nonlinearities in the CRF (compression and saturation) allow cortical cells to adjust the useful dynamic response to an operating range of contrast that can be modulated. This control is supposed to be adjusted by a dynamic balance between excitation and inhibition. The new parameters to adjust were the weight values of synaptic connections. At this point, it was done by hand, however, the next step is to adjust them by fitting experimental measurements from [16], with the same optimization algorithm previously described [15].

Figure 3 shows contrast response function of excitatory and inhibitory population of neurons, predicted by the model. The two CRF curves are very similar to those obtained electrophysiologically in [16].

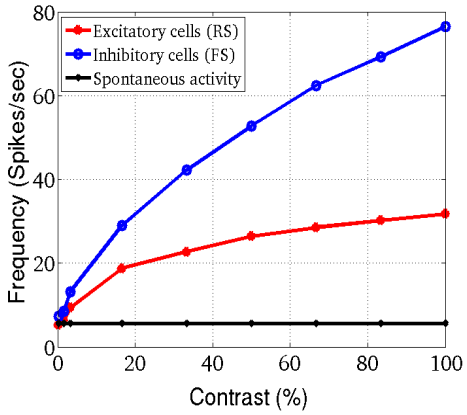

Figure 3. Contrast response function of excitatory (RS) and inhibitory (FS) population of neurons. The spontaneous activity has been plotted (black curve). Each point is the average of the mean firing rate for 13 repetitions of a given contrast.

3.2 Computation of the VSD signal

The VSD signal is simulated using a linear integration on the membrane surface of neuronal components. Here, the use of compartmental model has a real interest. Indeed, the computation of the VSD signal, for a given layer $\mathbf{L}$, is given by:

$$\mathbf{OI}^L = \lambda^L \sum_{i=0}^{N^L} \mathbf{V}_i(0.5)\,\mathbf{S}_i \qquad (2)$$

where

- N^L is the number of compartments in layer $\mathbf{L}$
- $\mathbf{S}_i$ is the surface of the ith compartment,
- $\mathbf{V}_i(0.5)$ is the membrane potential taken in the middle of the ith compartment,

- λ^L represents the fluorescence's gradient or the illumination intensity of the dye in layer **L**.

And then, the total optical imaging signal is given by the following formula:

$$\mathbf{OI} = \sum_{L \in \{Layers\}} \mathbf{OI}^L \tag{3}$$

Following this framework, we can simulate the VSD signal in response to known stimuli and compare it to experimental results [18]. We plotted the temporal evolution of the total VSD signal in response to an input of 600 ms and for different contrasts (see Figure 4).

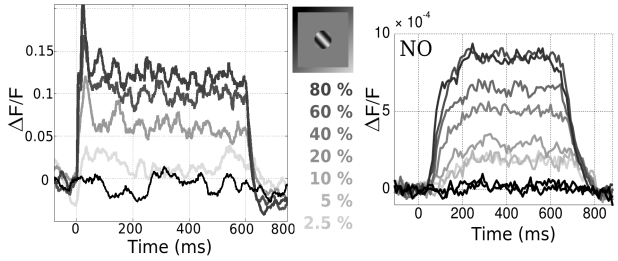

Figure 4. Temporal evolution of the VSD signal in response to an input of 600 ms and for several input contrasts. *Left*: Model, each curve is the average of the response for 50 repetitions of a given contrast. *Right*: VSDI experiment on monkey.

We also plotted the total VSD signal (in term of relative fluorescence: $\frac{\mathbf{\Delta F}}{\mathbf{F}}$) in function of input contrast (see Figure 5).

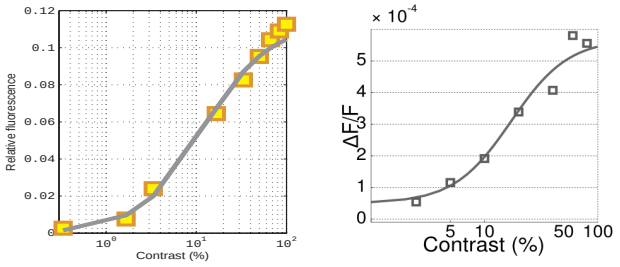

Figure 5. Total VSD signal in function of input contrast. *Left*: Model, each point is the average of the total response for 20 repetitions of a given contrast. *Right*: VSDI experiment on monkey.

The significance of the model is then demonstrated by comparing our results with the same curves obtained experimentally on monkey with VSDI (see right panels in figures 4 and 5).
However, Figure 4 shows a difference in time course between the model (left panel) and the experimental result (right panel). Indeed, the time course observed by the model is faster than the real one, showing that the model needs other adjustements to be completely realistic.

3.3 Contributions of the VSD signal

Our model can predict the different contributions of the VSD signal (see Figure 6):

- Excitation versus Inhibition: globally, excitatory cells are responsible of 80 percent of the total OI response, and inhibitory cells participation represents 20 percent of the OI signal. The ratio between excitation and inhibition shown in Figure 7 (Left panel) is weakly decreasing with contrast.
- Post-Synaptic activity versus Spiking activity: globally, only 75 percent of the optical signal comes from dendritic post-synaptic activity. The ratio between dendritic and axonic activity shown in Figure 7 (Middle panel) is weakly decreasing with contrast.
- Upper layers versus Lower layers: the optical signal is mostly originate from layers 2/3, but about 20 percent of the signal in layer 2/3 is from dendrites in deep layers. The ratio between upper and lower layers shown in Figure 7 (Right panel) is relatively constant with contrast.

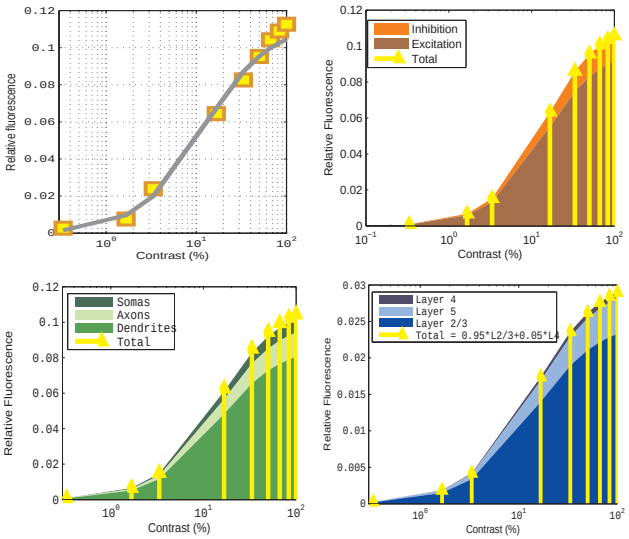

Figure 6. VSD responses in function of contrast showing the different contributions of the VSD signal. *Up Left*: Total OI response. *Up Right*: Excitation and inhibition contribution. *Down Left*: Somas, axons and dendrites contribution. *Down Right*: Layers contribution.

4 Conclusion

This model confirms and quantifies the fact that the VSD signal mainly reflects dendritic activity of excitatory neurons in superficial layers. However, the model also shows that inhibitory cells, spiking activity and deep layers are non-negligible and should be taken into account in the computation of the optical signal.

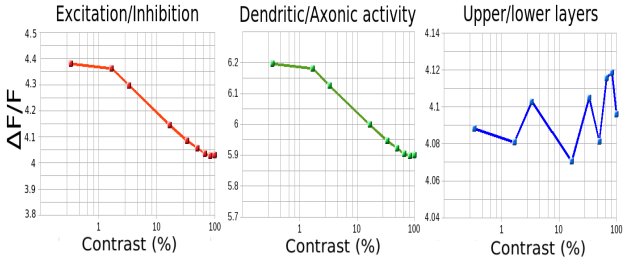

Figure 7. Rationale of the model. *Left*: Ratio between excitatory and inhibitory cells. *Middle*: Ratio between synaptic (dendritic) and spiking (axonic) activity. *Right*: Ratio between upper and lower layers.

5 Acknowledgments

The authors are especially grateful to Alain Destexhe for helpful discussions, in particular regarding the choice of parameters of the model.
This work is realized within the scope of the European FACETS project.

References

[1] A. Grinvald and R. Hildesheim. Vsdi: A new era in functional imaging of cortical dynamics. *Nature*, 5:874–885, nov 2004.

[2] C.C.H. Petersen and B. Sakmann. Functional independent columns of rat somatosensory barrel cortex revealed with voltage-sensitive dye imaging. *The journal of Neuroscience*, 21(21):8435–8446, nov 2001.

[3] V.B. Mountcastle. Modality and topographic properties of single neurons of cat's somatosensory cortex. *Journal of Neurophysiology*, 20:408–434, 1957.

[4] D.H. Hubel and T.N. Wiesel. Receptive fields, binocular interaction and functional architecture in the cat visual cortex. *J Physiol*, 160:106–154, 1962.

[5] D.H. Hubel and T.N. Wiesel. Receptive fields and functional architecture in two nonstriate visual areas (18 and 19) of the cat. *Journal of Neurophysiology*, 28:229–289, 1965.

[6] D.H. Hubel and T.N. Wiesel. Functional architecture of macaque monkey. *Proceedings of the Royal Society, London [B]*, pages 1–59, 1977.

[7] J.C. Horton and D.L. Adams. The cortical column: a structure without a function, April 2005.

[8] S. Haeusler and W. Maass. A statistical analysis of information-processing properties of lamina-specific cortical microcircuits models. *Cerebral Cortex*, 17:149–162, jan 2007.

[9] L. G. Nowak, R. Azouz, M. V. Sanchez-Vives, C.M. Gray, and D.A. McCormick. Electrophysiological classes of cat primary visual cortical neurons in vivo as revealed by quantitative analyses. *J Neurophysiol*, 89:1541–1566, mar 2003.

[10] P.C. Bush, D.A. Prince, and K.D. Miller. Increased pyramidal excitability and nmda conductance can explain posttraumatic epileptogenesis without disinhibition: A model. *Journal of Neurophysiology*, 82:1748–1758, 1999.

[11] T. Binzegger, R.J. Douglas, and K.A.C. Martin. A quantitative map of the circuit of cat primary visual cortex. *The Journal of Neuroscience*, 24(39):8441–8453, September 2004.

[12] A.M. Thomson and C. Lamy. Functional maps of neocortical local circuitry. *Frontiers in Neuroscience*, 1(1):19–42, nov 2007.

[13] A. Destexhe, M. Rudolph, J.M. Fellous, and T.J. Sejnowski. Fluctuating synaptic conductances recreate in-vivo-like activity in neocortical neurons. *Neuroscience*, 107:13–24, 2001.

[14] M.L. Hines and N.T. Carnevale. The neuron simulation environment. *Neural Computation*, 9:1179–1209, 1997.

[15] R. Brent. *A new algorithm for minimizing a function of several variables without calculating derivatives*, pages 200–248. Englewood Cliffs, NJ : Prentice Hall, 1976.

[16] D. Contreras and L. Palmer. Response to contrast of electrophysiologically defined cell classes in primary visual cortex. *Journal of Neuroscience*, 23(17):6936–6945, 2003.

[17] D.G. Albrecht and D.B. Hamilton. Striate cortex of monkey and cat: contrast response function. *Journal of Neurophysiology*, 48(1):217–233, jul 1982.

[18] A. Reynaud, F Barthelemy, GS Masson, and F Chavane. Input-ouput transformation in the visuo-oculomotor network. *Arch Ital Biol*, 145, 2007.